PROCEEDINGS OF SCIENCE

ATLAS Muon Trigger Performance

Robin Hayes*, **on behalf of the ATLAS Collaboration**
TRIUMF, University of British Columbia, Canada
E-mail: robin.hayes@cern.ch

Events containing muons in the final state are an important signature for many analyses being carried out at the Large Hadron Collider, including both Standard Model measurements and searches for new physics. To be able to study such events, it is required to have an efficient and well-understood muon trigger. The ATLAS muon trigger consists of a hardware-based system (Level 1), as well as a software-based reconstruction (High Level Trigger). Due to the high luminosity in Run 2, several improvements have been implemented to keep the trigger rate low while still maintaining a high efficiency. Some examples of recent improvements include requiring coincidence of hits in the muon spectrometer and the calorimeter and optimised muon isolation. We will present an overview of the muon trigger system, recent improvements, the performance of the muon trigger in Run 2 data and an outlook for the improvements planned for Run 3.

7th Annual Conference on Large Hadron Collider Physics - LHCP2019
20-25 May, 2019
Puebla, Mexico

*Speaker.

PoS(LHCP2019)007

1. Introduction

The trigger system at the ATLAS experiment [1] selects events that contain potentially interesting physics out of the enormous number of proton-proton collisions at the Large Hadron Collider (LHC), allowing these to be stored for later analysis. Many physics processes of interest contain muons in the final state, so triggering on events with prompt muons is crucial for the physics programme at ATLAS. Muon triggers are used in searches for massive vector bosons and precision tests of the Standard Model, among many other analyses, and were instrumental in the discovery of the Higgs boson.

In order to cope with the higher instantaneous luminosity and centre-of-mass energy in Run 2 (2015-2018) compared to Run 1 (2009-2013), the muon trigger system underwent several improvements over the course of Run 2. An overview of these upgrades and of the additional ones planned for Run 3 (2021-2023) is presented here.

2. The ATLAS Muon Spectrometer

The ATLAS muon trigger relies on information from the inner detector (ID) and the muon spectrometer (MS). The ATLAS MS sits in an average magnetic field of 0.5 T generated by three superconducting toroids and consists of four sub-detectors. The Thin Gap Chambers (TGC, $1.05 < |\eta| < 2.4$) and Resistive Plate Chambers (RPC, $|\eta| < 1.05$) are used for fast detector read-out for the trigger decision at Level-1 and offer position resolution on the order of mm. The Monitored Drift Tubes (MDT, $|\eta| < 2.7$) and Cathode Strip Chambers (CSC, $2.0 < |\eta| < 2.7$) have longer response times but provide position resolution on the order of 100 μm and are used for precision tracking. Figure 1 shows a quarter of a cross-section of the ATLAS muon system. The central region of ATLAS is called the barrel ($|\eta| < 1.05$), and the forward regions are called the endcaps ($|\eta| > 1.05$).

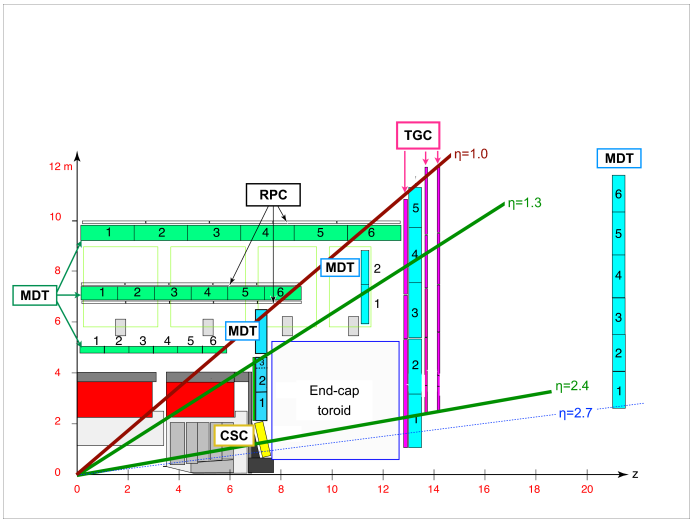

Figure 1: A quarter of a cross-section of the muon spectrometer in a plane containing the beam axis, showing the four sub-detectors of the MS: the Thin Gap Chambers (TGC), Resistive Plate Chambers (RPC), Monitored Drift Tubes (MDT) and Cathode Strip Chambers (CSC) [2].

3. The ATLAS Muon Trigger

The ATLAS trigger system consists of two levels. Level-1 (L1) triggers are hardware-based. Information from the L1 muon system and L1 calorimeter system is used by the Central Trigger Processor to make the L1 decision on whether to reject an event or to keep it for further processing, reducing the event rate from 40 MHz to 100 kHz. The L1 latency is approximately 2.5 μs. If a decision to keep an event is made at L1, then a Region-of-Interest (RoI) in the detector is passed to the High-Level Trigger (HLT), which refines the L1 decision using algorithms and tools that are similar to the ones used in offline reconstruction [3]. The HLT reduces the event rate to around 1 kHz with a latency of approximately 200 ms.

The muon trigger forms part of the ATLAS trigger system, and as such it can also be divided into two levels. At L1, the ATLAS muon trigger uses coincidences of hits in sublayers of the TGC or RPC of the MS to select muon candidates. The number of coincidences required depends on the p_{T} of the muon, which is estimated using a look-up table. RoIs identified at L1, which are typically 0.1 x 0.1 (0.03 x 0.03) in $\Delta\eta$ x $\Delta\phi$ in the RPC (TGC), are then passed on to the HLT. In a first "fast" stage, the HLT constructs MS-only muon candidates based on MDT information in addition to RPC and TGC hits. Their trajectory is identified by algorithms that use MDT drift times, and their p_{T} is calculated with empirical formulas. Then tracks in the MS are back-extrapolated to the interaction point, matched to an ID track, and combined with an ID track to form a combined muon track candidate. In regions covered by the CSC, hits in the CSC are used to refine the p_{T} estimate. A "precision" stage follows, in which offline muon reconstruction tools are used to precisely reconstruct muons. This stage is usually RoI-based but can also be run in full-scan mode, in which case track-finding is carried out in the full detector without using information from previous steps. Full-scan mode increases efficiency but is CPU-intensive.

4. Improvements to the Muon Trigger in Run 2

Run 2 featured higher instantaneous luminosities, centre-of-mass energy and pileup (number of collisions per proton bunch crossing) than Run 1, all of which contributed to a higher rate of events. In order to contend with this higher rate without sacrificing the ATLAS physics programme, several upgrades to the muon trigger were made.

4.1 Level-1 Trigger

Trigger efficiency in the barrel ($|\eta| < 1.05$) is lower than in the endcaps because L1 trigger coverage is limited by the barrel support structures. In 2016, new RPCs covering these gaps were commissioned and installed. This led to a 20% efficiency increase in the exact regions covered by the new RPCs, and a 4% efficiency increase across the whole barrel. Figure 2 shows the impact of the new chambers on L1 trigger efficiency in one of the support structure regions.

In the endcaps, requiring 3-station rather than 2-station coincidences of hits in certain TGC channels lowered the rate of L1 triggers that require two and three L1 muons with $p_{\mathrm{T}} > 4$ GeV without reducing efficiency, as shown in Figure 3. This adjustment also reduced the rate dependence on pileup.

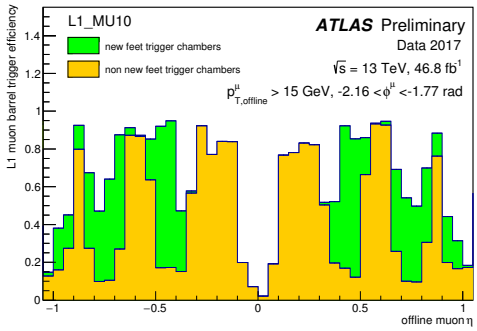

Figure 2: The impact of the new RPC trigger chambers on the efficiency of the L1_MU10 trigger [4].

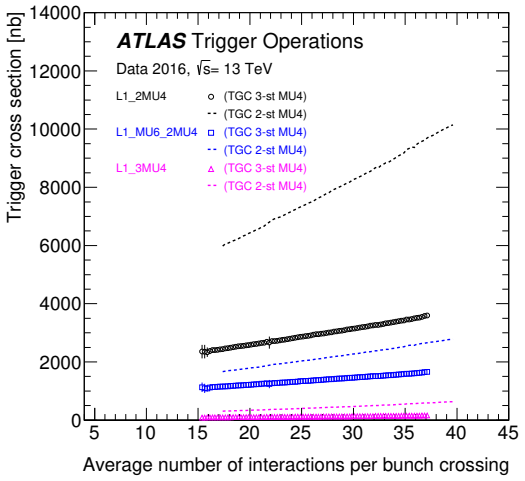

Figure 3: Trigger cross-sections with different TGC coincidence requirements, as a function of the number of interactions per bunch-crossing [5].

Several optimizations during Run 2 also contributed to lower trigger rates in the endcaps. In 2017, the overlap region of the barrel feet and the spatial Coincidence Window (CW) requirement were optimized using 2016 data, resulting in an overall rate reduction for the L1_MU20 trigger in 2017 as shown in Figure 4.

Optimization of the CW also reduced the L1_3MU4 rate in 2018 by 7%, which is shown in Figure 5.

Finally, a set of muon trigger upgrades were motivated by the need to minimize the fake rate. For $|\eta| > 1.05$, the L1 muon trigger rate is dominated by fakes. These are mostly attributed to low-energy particles, generated mainly in the endcap toroid, that hit the L1 trigger chambers at a similar angle to high-p_{T} muons [6]. To discriminate real muons from fakes, additional trigger chamber coincidence requirements were imposed during Run 2. First, an additional coincidence between the TGCs of the MS Big Wheel and the inner muon chambers placed before the endcap toroid (the Forward Inner (FI) chambers at $1.3 < |\eta| < 1.9$ and Endcap Inner (EI) chambers at $1.05 < |\eta| < 1.3$) was adopted beginning in 2015 (FI) and 2016 (EI). This reduced the L1_MU20 rate by 20% with an efficiency loss of just 1%. Next, a coincidence between the Big

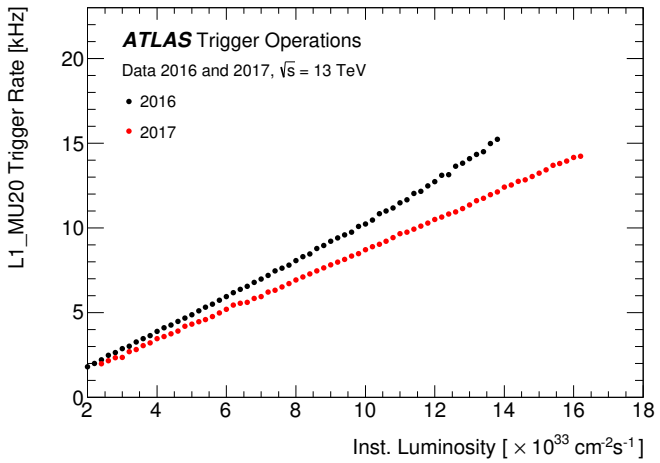

Figure 4: Impact of several data-driven optimizations on the L1_MU20 trigger rate in 2017. [4].

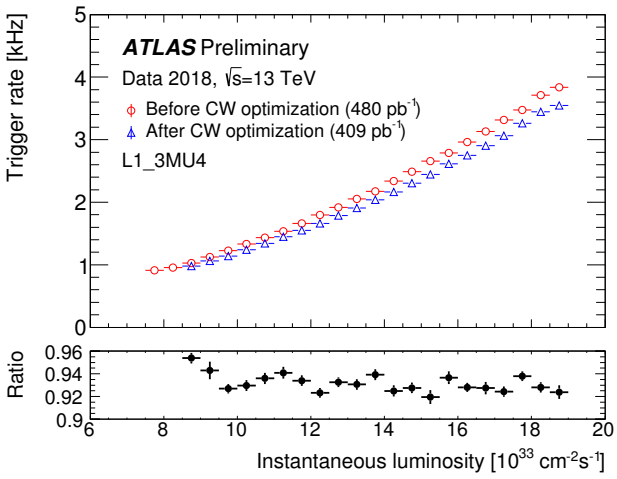

Figure 5: Impact of data-driven Coincidence Window optimization on the L1_3MU4 trigger rate [4].

Wheel TGCs and the tile calorimeter was imposed for muons at $1.05 < |\eta| < 1.3$. This reduced the L1_MU20 rate by an additional 6%, with negligible efficiency loss. Figures 6 and 7 show the impacts of these changes on the L1_MU20 rate across the entire $|\eta|$ range of the MS.

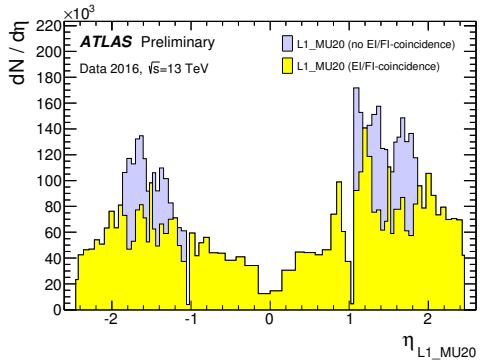

Figure 6: Rate reduction of the L1_MU20 trigger due to the inner muon chamber coincidence requirement. [5].

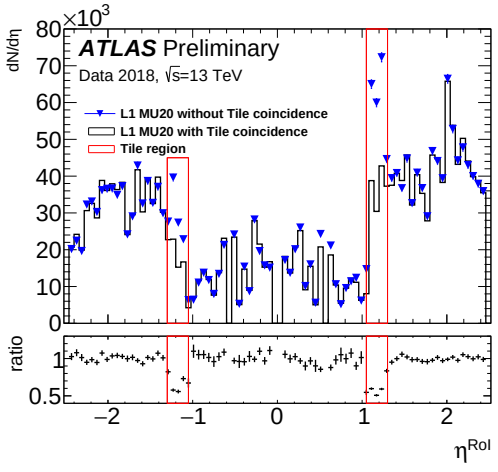

Figure 7: Rate reduction of the L1_MU20 trigger due to the tile calorimeter coincidence requirement. [4].

4.2 High-Level Trigger

Run 2 conditions also motivated some improvements to the HLT. Some muon trigger algorithms involve cuts on the so-called isolation of a muon candidate. Isolation is calculated as the scalar sum of the p_T of tracks in a cone around the muon track. Tracks that originate a certain distance from the muon, labelled dz, are first excluded from the cone. In 2016, a new isolation criterion called "ivarmedium" with an optimized cone size was introduced, replacing the previous "iloose" for use in the primary trigger. In the high-pileup conditions of 2017, it was observed that

the lowest-p_{T} unprescaled isolated single-muon trigger suffered a loss in efficiency. In response, the dz cut was tightened from 6 mm to 2 mm in 2018. This excludes more pileup tracks from the cone in which isolation is calculated, and makes it more likely that muons will pass the trigger's isolation requirement. This successfully recovers efficiency, increasing it from 96% to 99% at an average pileup of 60, with only a modest (16 Hz) increase in rate [7].

Improving the resolution of the p_{T} estimate performed at HLT helps to refine the muon trigger decision and steepen the trigger turn-on curve, improving efficiency and reducing background. To this end, additional hit information from the CSC chambers ($2.0 < |\eta| < 2.4$) and Extended Endcap (EE) chambers ($1.05 < |\eta| < 1.35$) was included in the HLT fast algorithm. Figure 8 shows the resulting improvement in the p_{T} resolution of this algorithm.

Finally, various improvements were made to reduce noise and fakes, and to decrease processing time. These include imposing a drift-length cut in track construction performed in the HLT fast step to remove fake signals and optimising algorithm call sequences to improve performance in the HLT precision step.

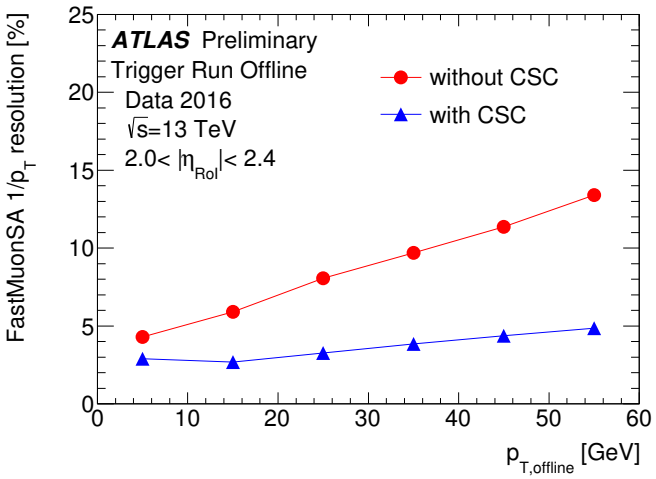

Figure 8: Inverse-p_{T} resolution of the algorithm that calculates muon p_{T} for the HLT decision, as a function of muon offline p_{T} [5].

5. Muon Trigger Efficiency

In order to evaluate the performance of the muon trigger, the tag-and-probe method is employed to measure trigger efficiency. $Z \to \mu\mu$ decays are used to provide a clean signature for this method. One muon from the decay is identified as the tag. Triggering on the tag using a loose trigger creates an unbiased pool of events from which trigger efficiency can be measured. The other muon in the decay serves as the probe as long as it passes several selections. Trigger efficiency is measured as the fraction of probe muons that are matched in ΔR to an object that caused the probe trigger to fire. For low-p_{T} triggers, the J/ψ topology is used instead. High-p_{T} trigger efficiency is evaluated using W+jets or $t\bar{t}$ events, in which case the tag is $E_{\mathrm{T}}^{\mathrm{miss}}$.

The efficiency of an exemplary HLT and the L1 trigger from which it is seeded is shown in Figure 9 for the barrel and Figure 10 for the endcaps. The L1 trigger efficiency is mostly determined by physical coverage of the detector, and is lower in the barrel ($\sim 80\%$ coverage) than in the endcaps ($\sim 99\%$ coverage). The HLT efficiency is nearly 100% relative to L1.

6. Muon Trigger Upgrades for Run 3

In Run 3, background rates will continue to present a challenge. To cope with this, the muon

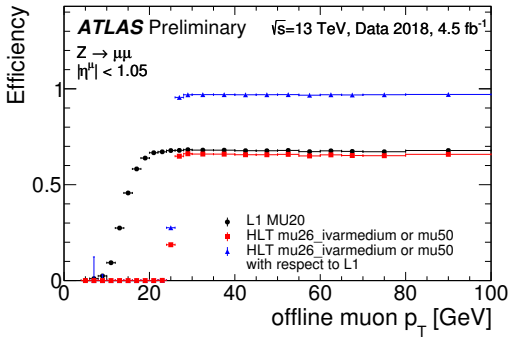

Figure 9: Trigger efficiency of HLT and L1 triggers as a function of offline muon p_{T} in the barrel [5].

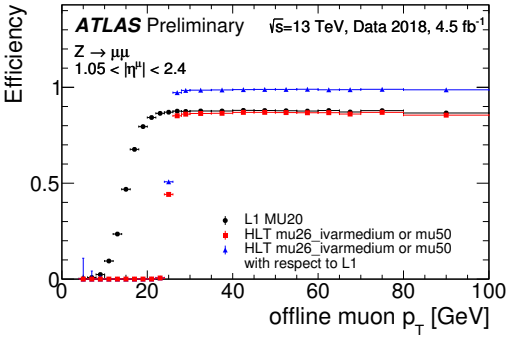

Figure 10: Trigger efficiency of HLT and L1 triggers as a function of offline muon p_{T} in the endcaps [5].

trigger system will undergo several upgrades. A new layer of integrated small-MDT (sMDT) and thin-gap RPC detectors has been installed in a portion of the MS. These cover acceptance gaps created by the service elevator in the barrel and have reduced occupancy because of their small size, which leads to better resolution and lower background rates.

New Small Wheels (NSW) will replace the existing small wheels of the endcaps. The NSW will be instrumented with small-TGC (sTGC) and MicroMegas (MM) detector technologies. It will offer 1 mrad angular resolution and improved detector coverage. Requiring coincidences with the NSW rejects tracks due to particles that do not originate from the interaction point. The NSW is projected to reduce the L1 muon trigger rate by 50%. Figure 11 compares the number of muon candidates with Run 2 coincidence requirements and with several coincidence logics involving the NSW.

7. Conclusion

Thanks to several key upgrades, the muon trigger system has performed well throughout LHC Run 2. The challenging data-taking conditions of Run 3 will further test its ability to efficiently select muons while rejecting enough fakes to achieve reasonable trigger rates. The improvements planned for Run 3 will ensure that the muon trigger can continue to play a crucial part in meeting the demands of the ATLAS physics programme.

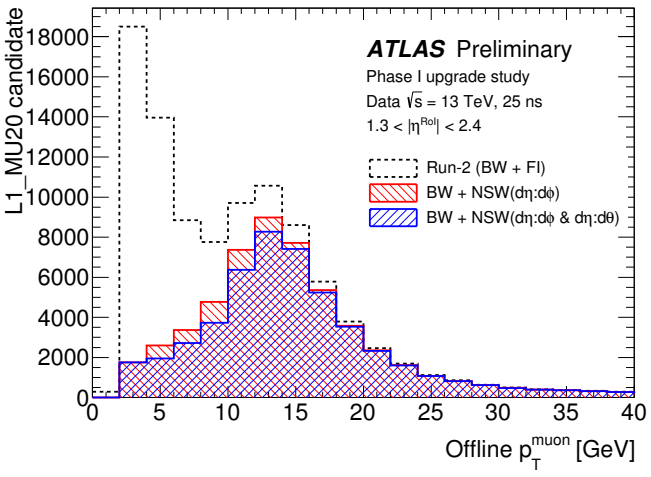

Figure 11: Number of L1_MU20 candidates selected when coincidences of hits in the Big Wheel TGCs (BW) and Forward Inner TGCs (FI) are required, compared to the number selected when various coincidence logics are applied to the BW and NSW [4].

References

[1] ATLAS Collaboration, *The ATLAS Experiment at the CERN Large Hadron Collider*, JINST **3** S0800 (2008)

[2] ATLAS Collaboration, *Performance of the ATLAS muon trigger in pp collisions at* $\sqrt{s}$*=8 TeV*, Eur. Phys. J. C **75** (2015) 120 [hep-ex/1408.3179].

[3] ATLAS Collaboration, *Performance of the ATLAS Trigger System in 2015*, Eur. Phys. J. C **77** (2017) 317 [hep-ex/1611.09661].

[4] ATLAS Collaboration, *L1 Muon Trigger Public Results*, https://twiki.cern.ch/twiki/bin/view/AtlasPublic/L1MuonTriggerPublicResults, 2018.

[5] ATLAS Collaboration, *Muon Trigger Public Results*, https://twiki.cern.ch/twiki/bin/view/AtlasPublic/MuonTriggerPublicResults, 2018.

[6] ATLAS Collaboration, *ATLAS New Small Wheel Technical Design Report* (2013) http://inspirehep.net/record/1615722/references?ln=en

[7] S. Hayashida, *The ATLAS Muon Trigger*, in proceedings of *23rd International Conference on Computing in High Energy and Nuclear Physics* (2018) ATL-DAQ-PROC-2018-039 https://cds.cern.ch/record/2649074?ln=en.